


# Role of water in intramolecular proton transfer reactions of formamide and thioformamide

Daniela Guzmán-Angel<sup>1</sup> · Ricardo Inostroza-Rivera<sup>2</sup>  · Soledad Gutiérrez-Oliva<sup>1</sup> · Bárbara Herrera<sup>1</sup> · Alejandro Toro-Labbé<sup>1</sup>

Received: 29 August 2015 / Accepted: 30 November 2015  
© Springer-Verlag Berlin Heidelberg 2016

**Abstract** A theoretical study of the mechanism of intramolecular proton transfer reactions in formamide and thioformamide is presented; the focus is on the characterization of the role of water in the reactions. The reaction mechanisms was analyzed with the help of energy profiles in the frame of the reaction force analysis and using the reaction electronic flux to characterize the electronic activity that takes place along the reaction. Bader's quantum theory of atoms in molecules is used to confirm the reaction mechanism and help elucidate the specific role of water. Results at the DFT/B3LYP 6-311G\*\* level of theory show that water catalyzes the proton transfer reaction lowering the activation energy by a factor of two. The reaction force analysis allowed the characterization of activation energies, indicating that in all four reactions, it is mostly due to structural reordering.

## 1 Introduction

Proton transfers (PT) are one of the most fundamental processes in chemistry and biology [1–3]. Multiple-proton transfer reactions that can occur synchronously or

asynchronously include proton relay systems in enzymes, hydrogen-bonded water complexes, prototropic tautomerism and tautomerism in DNA bases. Proton transfer reactions in formamide and thioformamide are important reactions since the functional groups forming these molecules play important roles in chemistry, biology and pharmacy. The amide group has a fundamental role as a basic building block of proteins and enzymes; it is characterized by some specific properties like coplanarity of the groups attached to the nitrogen atom, high rotational barrier and kinetic stability toward nucleophilic attack or hydrolysis [4, 5]. These are therefore model PT reactions for more complex chemical processes taking place in proteins and nucleic bases [6, 7].

Intramolecular proton transfer (iPT) takes place within a molecule in which both donor and acceptor atoms are concerted to achieve the processes [7–9]. The effect of water as a catalyst in proton transfer reactions is a well-known and well-studied phenomenon [6, 8, 10–14]; water molecule acts as a linker between the donor and acceptor atoms. As a result, it may stabilize the transition state, thus leading to a decrease in the energy barrier. In water-mediated PT reactions, the TS structure is stabilized by four hydrogen bonds [6, 7, 10, 11] in contrast with iPT where the TS structure has only two hydrogen bonds [7, 8].

In this work, we have studied the mechanism of intramolecular proton transfer reactions in formamide and thioformamide; the focus is on the role of water molecule as a catalyst. So two different kinds of processes will be analyzed in this paper, iPTs taking place in formamide and thioformamide and the corresponding water-mediated processes (wPT). The density functional theory (DFT) descriptors will be used to help characterize the reaction mechanism of the intramolecular proton transfer of formamide and thioformamide. The reactions will be studied using the reaction force analysis [15–22] that defines a framework to

Published as part of the special collection of articles “CHITEL 2015 - Torino - Italy”.

✉ Ricardo Inostroza-Rivera  
rjinostr@uc.cl

<sup>1</sup> Nucleus Millennium Chemical Processes and Catalysis (CPC), Laboratorio de Química Teórica Computacional (QTC), Departamento de Química Física, Facultad de Química, Pontificia Universidad Católica de Chile, Av. Vicuña Mackenna 4860, 76220436 Macul, Santiago, Chile

<sup>2</sup> Facultad de Ciencias de la Salud, Universidad Arturo Prat, Casilla 121, 1110939 Iquique, Chile

characterize chemical events taking place at different steps of the reaction and allows to quantify the energy involved at each step along the reaction. The electronic activity taking place during the chemical reaction will be characterized using the reaction electronic flux (REF) [20–25]. Finally, for a closer view of the changes in electron density during the reaction, Bader's quantum theory of atoms in molecules (QTAIM) will be used [26–30].

This paper is organized as follows: In the next section, we present the theoretical elements used in our analysis of the reactions. Section 3 describes the computational methods employed, and in Sect. 4, we present and discuss the results. Conclusions are drawn in Sect. 5.

## 2 Theoretical background

### 2.1 The reaction force

For a chemical process with energy profile  $E(\xi)$ , along the reaction coordinate  $\xi$ , the reaction force  $F(\xi)$  is defined as follows [15]:

$$F(\xi) = -\frac{dE}{d\xi} \quad (1)$$

For any elementary step, the reaction force is characterized by two critical points at  $\xi_1$  and  $\xi_2$  that provide a natural partitioning of the reaction coordinate into three regions: the reactants, transition state and products regions. Our experience in a large series of reactions [16–19] indicates that each region has certain factors that tend to dominate: In the reactant region (R) ( $\xi_R \leq \xi \leq \xi_1$ ), structural effects dominate, in the transition state region (TS) ( $\xi_1 \leq \xi \leq \xi_2$ ), electronic reordering prevails over structural effects, and in the product region (P) ( $\xi_2 \leq \xi \leq \xi_R$ ), structural arrangements again take over to allow relaxation that leads to the final equilibrium geometry of the products.

The reaction force analysis provides a natural decomposition of the activation and reaction energies,  $\Delta E^\ddagger$  and  $\Delta E^\circ$ , into different components that emerge from the above definition of reaction regions:

$$\begin{aligned} \Delta E^\ddagger &= [E(\xi_{\text{TS}}) - E(\xi_{\text{R}})] \\ &= W_1 + W_2 \end{aligned} \quad (2)$$

$$\begin{aligned} \Delta E^\circ &= [E(\xi_{\text{P}}) - E(\xi_{\text{R}})] \\ &= W_1 + W_2 + W_3 + W_4 \end{aligned} \quad (3)$$

where

$$\begin{aligned} W_1 &= -\int_{\xi_{\text{R}}}^{\xi_1} F(\xi) d\xi > 0 \\ W_2 &= -\int_{\xi_1}^{\xi_{\text{TS}}} F(\xi) d\xi > 0 \end{aligned} \quad (4)$$

$$\begin{aligned} W_3 &= -\int_{\xi_{\text{TS}}}^{\xi_2} F(\xi) d\xi < 0 \\ W_4 &= -\int_{\xi_2}^{\xi_{\text{P}}} F(\xi) d\xi < 0 \end{aligned} \quad (5)$$

are reaction works associated with processes occurring at every stage of the reaction. Therefore, activation and reaction energies can be characterized through the relative contributions of electronic and structural effects quantified by the reaction works defined in Eqs. (3) and (4).

### 2.2 Reaction electronic flux

DFT provide the theoretical framework for rationalizing chemical reactions in terms of the response of the molecular system toward the variation of the total number of electron ( $N$ ) and the external potential ( $v(r)$ ). The response to changes in  $N$ , when the  $v(r)$  remains constant, is measured at first order by the chemical potential ( $\mu$ ) [31, 32] which is related to the electronegativity ( $\chi$ ) of a system [31]:

$$\mu = \left( \frac{\partial E}{\partial N} \right)_{v(r)} = -\chi \quad (6)$$

Operational schemes for the calculation of  $\mu$  are based on the three-point finite-difference approximation to  $(\partial E)/(\partial N)$ ; this leads to an expression for the chemical potential in terms of the first ionization potential (IP) and the electron affinity (EA). Further approximation, using the Koopmans theorem [32], uses the energy of the HOMO and LUMO frontier molecular orbitals:

$$\mu \simeq -\frac{1}{2}(\text{IP} + \text{EA}) \simeq \frac{1}{2}(\varepsilon_{\text{H}} + \varepsilon_{\text{L}}) \quad (7)$$

Equation (7) provides a way to determine numerical values of  $\mu$ , all along the reaction coordinate, thus leading to  $\mu(\xi)$ . According to Eq. (7), a new concept emerges, the reaction electronic flux (REF) [20]:

$$J(\xi) = -\left( \frac{d\mu}{d\xi} \right) \quad (8)$$

The  $J(\xi)$  profile has been proven to be useful in the characterization of electronic activity that is actually taking place along the reaction coordinate. In analogy with thermodynamics, the changes in the chemical potential along the reaction coordinate [21, 22] can be interpreted as describing the spontaneity of electronic reordering processes that takes place during the reaction. For instance, positive values of REF will entail spontaneous changes in electronic density, indicating that bond strengthening or forming processes drive the reaction. In contrast to this, negative values of REF indicate non-spontaneous electronic reordering driven by weakening or bond-breaking processes [33].

### 3 Computational details

All the structures have been fully optimized using the *Becke-3* parameters for exchange and Lee–Yang–Parr functional for correlation [34–37] (B3LYP) with standard 6-311G\*\* basis set. The minimum energy path in going from reactants to products was calculated through the intrinsic reaction coordinate procedure (IRC) [38]. Frequency calculations on reactants, transition state and products were performed to confirm the nature of the corresponding critical points along the reaction path. All calculations were carried out using the Gaussian 09 program [39]. For the electron density topology analysis, the AIM-ALL software was used [40].

## 4 Results and discussion

### 4.1 Energy and reaction force profiles

Figure 1 shows the four reactions under study: the intramolecular proton transfer in formamide (iF) and thioformamide (iT) and the water-mediated proton transfers in formamide (wF) and thioformamide (wT). The energy and force profiles along the intrinsic reaction coordinate of all reaction are displayed in Figs. 2 and 3, respectively. The vertical lines displayed in Fig. 2 and in the forthcoming figures indicate the limits of the reaction regions that have been determined from the critical points of the reaction force profiles. Energetic parameters are displayed in Table 1.

The barriers for iPT indicate that the donor/acceptor atoms play a key role in the transfer, when sulfur is the accepting atom the barrier is 42.0 kcal/mol, lower than when oxygen is the acceptor atom (48.0 kcal/mol); this seems to be due to negative hyperconjugation between the lone pair of the nitrogen and the  $\sigma^*$  orbital of the S–H bond. This interaction stabilizes the transition state. In addition, it was found that both reactions are thermodynamically unfavorable, indicating that the amino form is more stable than the imino form; in iF, this seems to be due to the fact that the oxygen atom is a better hydrogen acceptor than sulfur atom. When the proton transfer reactions are assisted by a water molecule, the activation energies fall down dramatically reaching values of 21.3 kcal/mol for wF and 22.3 kcal/mol for wT. When we compare the energy barrier for the iPT and the wPT for the pair of systems {iF, wF} and {iT, wT}, the catalytic effect of water becomes apparent. This trend is also observed in reaction energies ( $\Delta E^\circ$ ); wPT reactions become less endothermic than their iPT analogues.

We have calculated the reaction works involved at each step along the reaction coordinate using Eqs. (4) and (5). In agreement with previous studies [15–22, 24, 25], the first

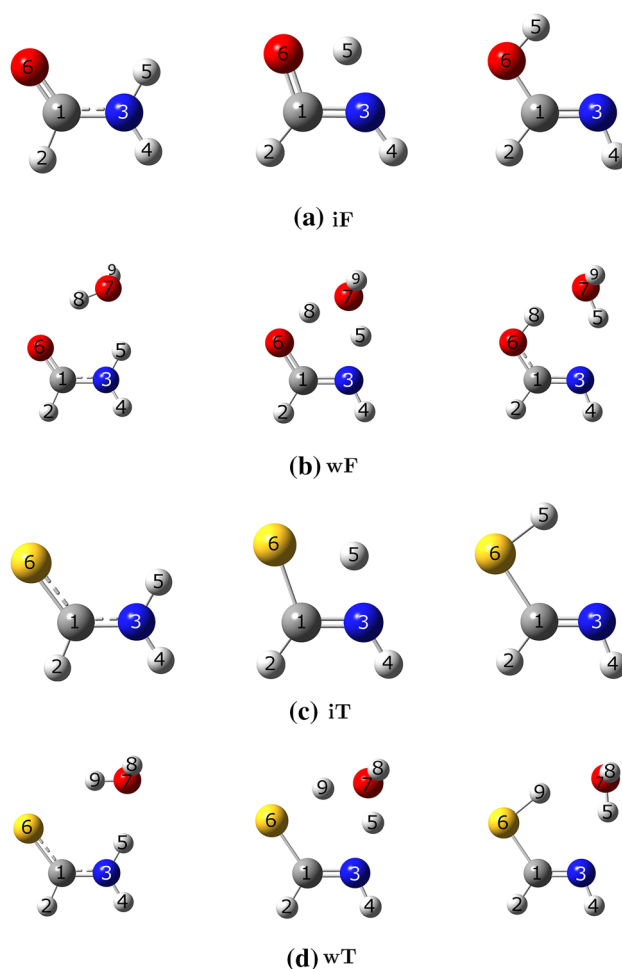


**Fig. 1** Reactions under study. The intramolecular proton transfer in formamide (iF) and thioformamide (iT) and water-mediated proton transfers in formamide (wF) and thioformamide (wT)

step of activation process of any elementary step is dominated mostly by structural rearrangements ( $W_1$ ), and the second step is dominated by rearrangements in the electronic density ( $W_2$ ). The intramolecular proton transfer reactions (iPT) present structural work  $W_1$  that corresponds to roughly 70 % of the energy barrier, showing that structural rearrangement drives the iPT reactions. For the proton transfer reactions assisted by a water molecule, wF and wT, the structural work  $W_1$  corresponds to 73 and 64 % of the energy barrier, respectively. We can see that water molecule decreases the reaction works ( $W_1$  and  $W_2$ ) needed to reach the transition state consistently by a factor of two, thus explaining the decrease in energy barriers.

It is interesting to note the net catalytic effect of the oxygen substitution by sulfur; almost 6 kcal/mol are gained in the iPT reaction, most of them associated with structural work  $W_1$ . In contrast to this, the wPT reaction does not show a catalytic effect due to substitutions; in fact, the energy barrier increase by 1 kcal/mol upon substitution of

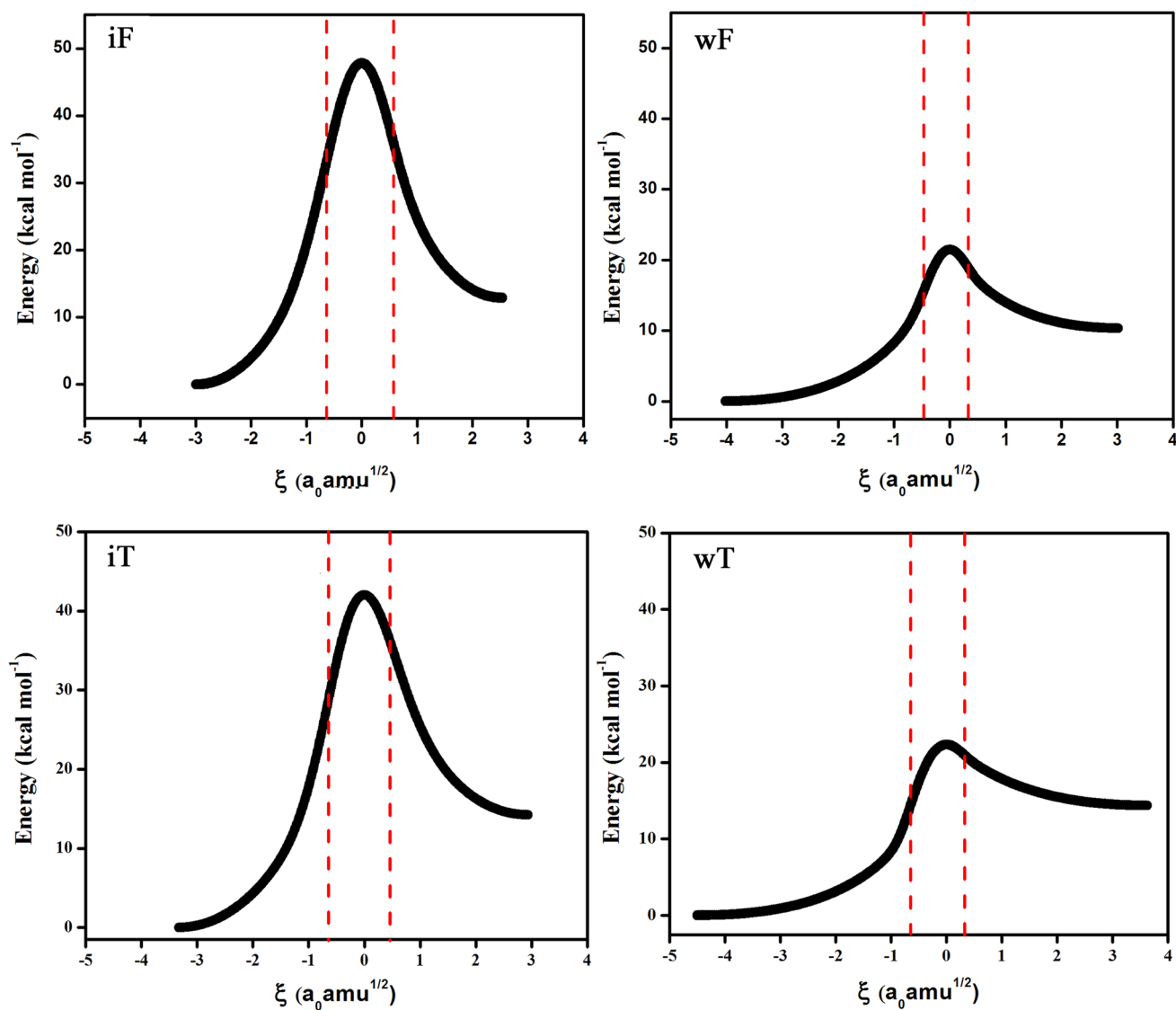


**Fig. 2** Energy profile (in kcal/mol) for each reaction

oxygen by sulfur. Concerning the reaction energies, the most noticeable change is observed in  $W_3$  and  $W_4$ ; their values drop down dramatically when water comes into play. The net result is a net lowering of reaction energies by few kcal/mol.

In summary, wPT reactions are kinetically more favorable, lowering considerably the energy barriers. Reaction energies are also favored by the presence of water molecule even though the reaction remains being endergonic processes.

#### 4.2 Reaction electronic flux

The REF profiles of reactions are displayed in Fig. 4; it can be noticed that iF and iT present a similar trend, quite constant at the reactant region, confirming that in this

region, structural rearrangements prevail; the REF profile indicates that most electronic activity takes place in transition state region. Finally, in the product regions, the electronic activity tends to equilibrate at small values of REF. iF and iT exhibit a large positive peak, spontaneous electronic activity [ $J(\xi) > 0$ ] associated with the ability of oxygen and sulfur to capture the proton. The intensity of the positive peak might be indicating that oxygen is a better hydrogen acceptor than sulfur. Afterward, a non-spontaneous electronic activity [ $J(\xi) < 0$ ] associated with bond weakening or breaking processes develops leaving the TS region. Broader and less intensive peaks characterize the REF profile of iT, indicating a long-lasting electronic activity.

On the other hand, wF shows a more peculiar behavior, a unique positive peak mostly located at the TS region

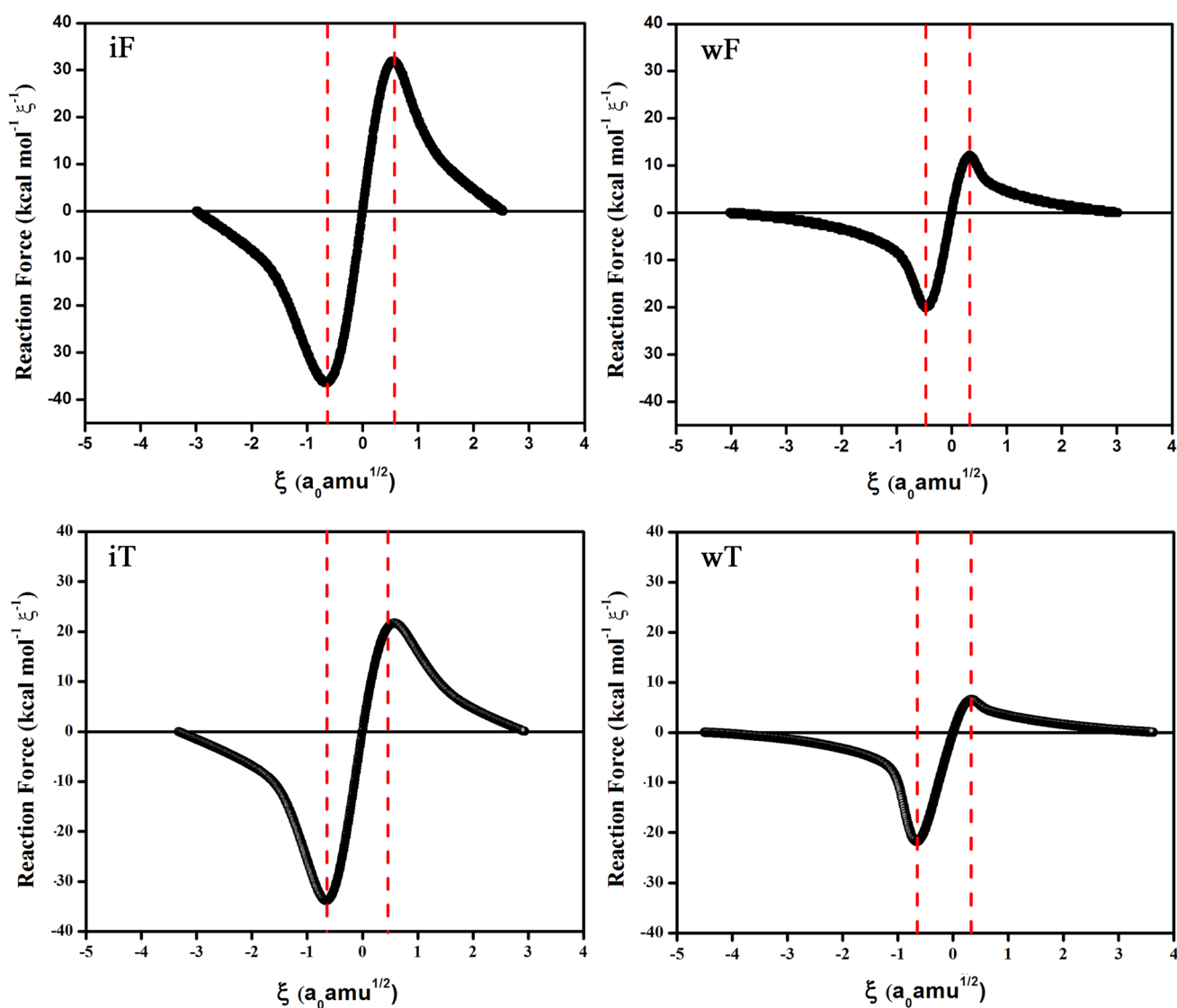


**Fig. 3** Reaction force profile (in kcal/mol) for each reaction

**Table 1** Reaction energy ( $\Delta E^\circ$ ), energy barrier ( $\Delta E^\ddagger$ ) and works associated with different systems, all values in kcal/mol

Reaction	$\Delta E^\ddagger$	$\Delta E^\circ$	$W_1$	$W_2$	$W_3$	$W_4$
iF	47.80	12.90	33.28	14.52	-11.67	-23.24
iT	42.00	14.23	28.67	13.33	-7.76	-20.01
wF	21.30	10.35	15.47	6.00	-2.53	-8.59
wT	22.32	11.57	14.29	8.03	-1.40	-9.35

indicating that spontaneous activity associated with the **O–H** bond-forming processes drives the reaction. On the other hand, wT present a REF profile quite similar to those presented by nucleophilic substitution reaction [41, 42], a pulse with a negative peak followed by a positive one, in which breaking of **N–H** and **O–H** bonds initially drives the reaction, but then the **O–H** and **S–H** formation processes takes over and signing the positive peak whose maximum

is found within the TS region. The REF profile for wT indicates that this reaction takes place following a stepwise mechanism.

### 4.3 Natural bond analysis

In order to analyze the nature of electron transfer for iF, iT, wF and wT systems, we analyze the bond electronic

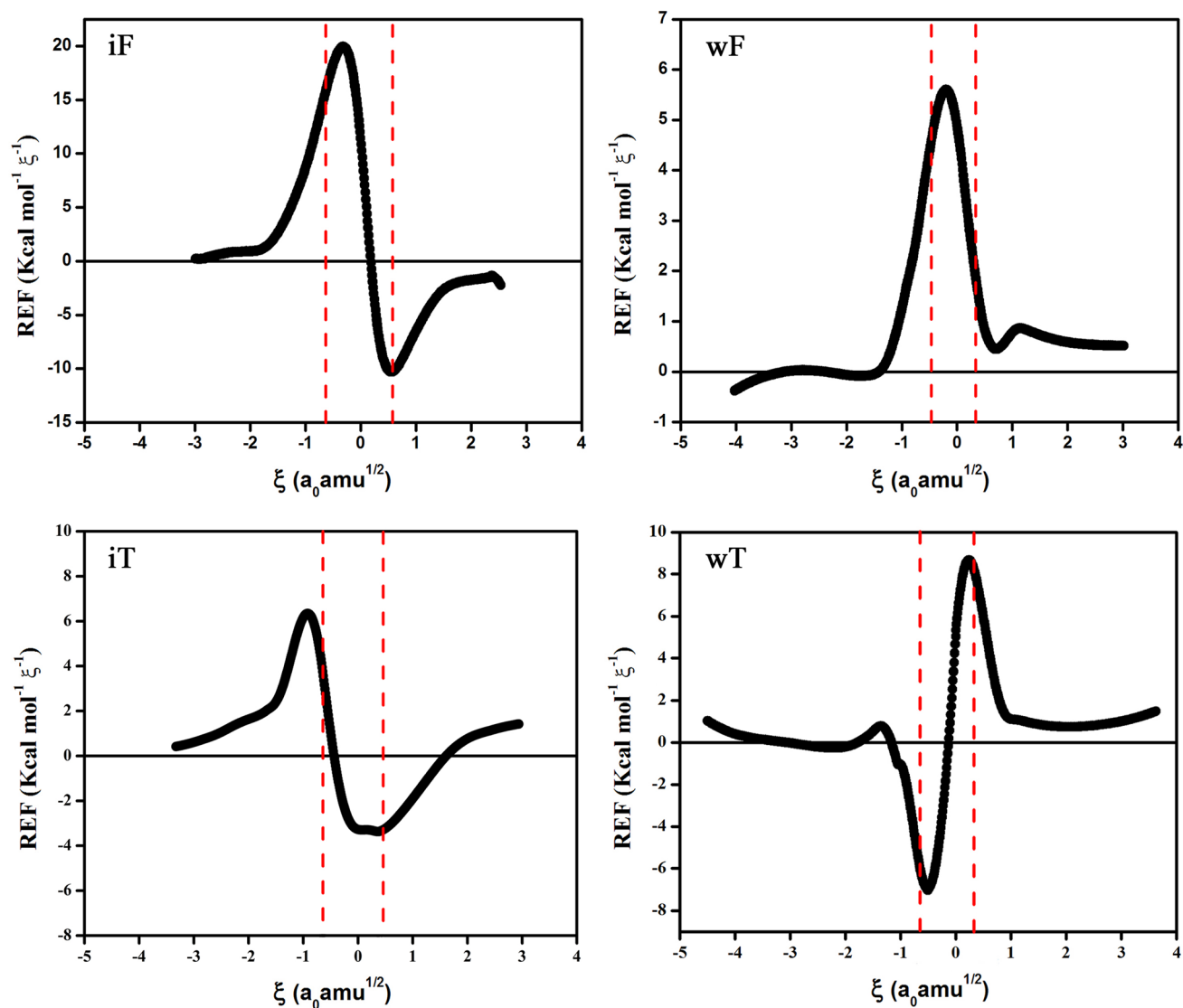


**Fig. 4** Reaction electronic flux (REF,  $J(\xi)$ ) profile (in kcal/mol) for each reaction

populations. Figure 5 shows the evolution of the derivatives of Wiberg bond order along the reaction coordinate for the four reactions. The use of derivatives of bond order has been quite useful to characterize changes in bond population and has been validated through its relationship with the REF [43]. It can be seen that the highest intensity of bond order reordering takes place at the transition state region, as it was indicated by the electronic flux.

Figure 5 shows that the **N3H5** a **iF** bond dissociation occurs simultaneously with the formation of **O6H5** bond. Also the breaking of the **C1O6** double bond is in phase with the formation of the **C1N3** double bond being a clear indicator of a synchronic proton transfer. Similarly, the **N3H5** at **iT** bond breaking is in phase with the formation of **S6H5** bond, whereas the weakening of **C1S6**

occurs simultaneously with the **C1N3** strengthening, also indicating that the breaking/forming processes take place synchronously.

For the **wF** proton transfer reaction, **O7H5** and **O6H8** bond formations drive the reaction and a single positive peak signs the REF profile. This is because oxygen is a good proton acceptor and thus facilitates the **N3H5** bond breaking and activates the transfer of **H8** from water. This determines that the electron transfer at the transition state is occurring synchronically. On the other hand, in **wT** **N3H5** bond breaking and **O7H5** bond formation drive the reaction at the TS region although the breaking process prevails to define the first negative peaks in the REF profile (Fig. 4). Then, **S6H9** bond formation produces the positive peak of the REF and drives the remaining reaction. All this

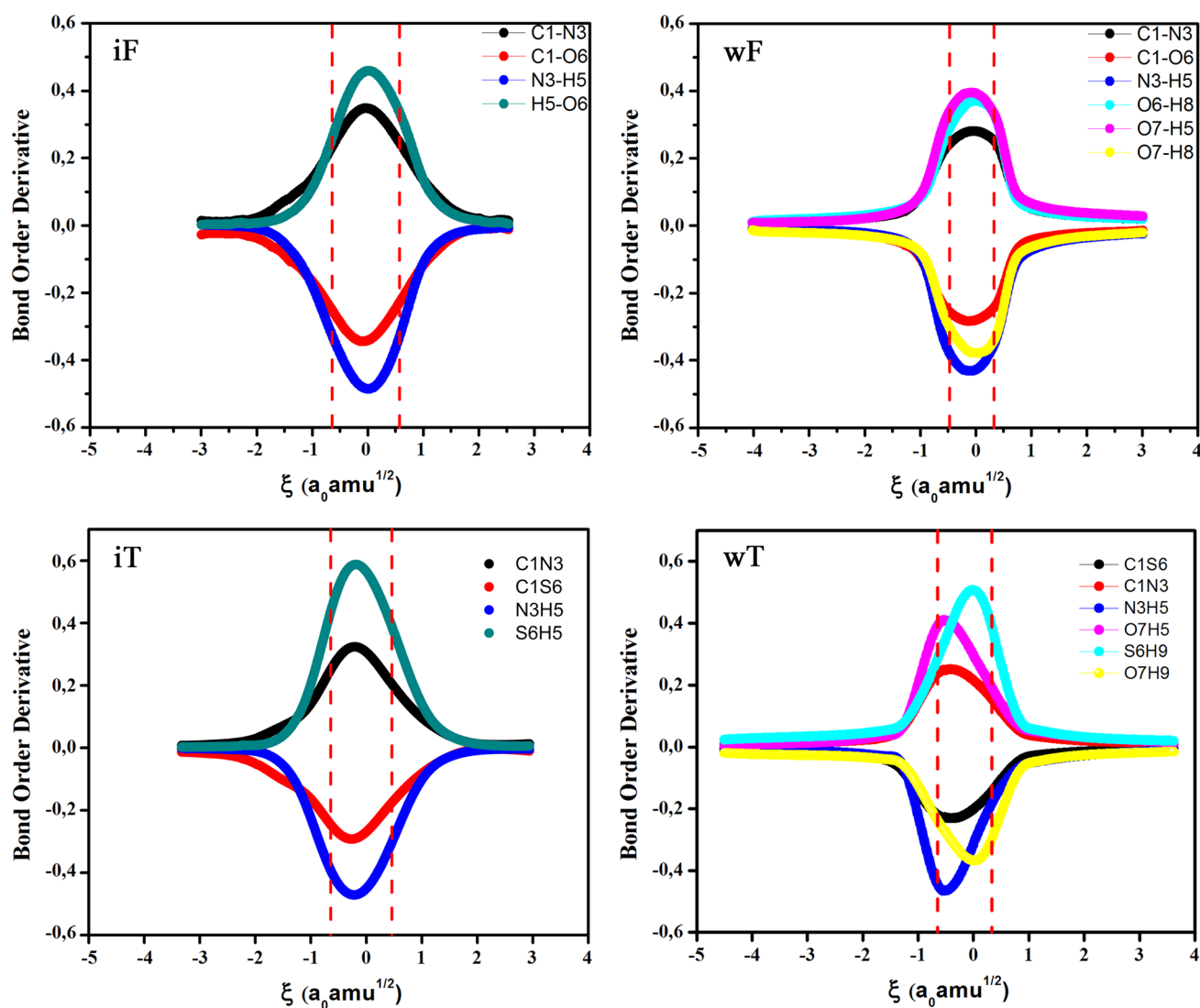


**Fig. 5** Derivates of bond order (in a.u.) for the proton transfer reaction in iF, iT, wF and wT

indicates that the breaking/forming processes take place slightly asynchronously.

#### 4.4 Electron transfer from QTAIM point of view: topology of the electron density

In order to analyze the nature of the electron transfer, we analyze the electron density topology; Fig. 6 shows the evolution of electron density at the selected (3, -1) and (3, +1) critical points along the intrinsic reaction coordinate in iF and wF (for iT and wT, the same behavior was observed). At the beginning, the transferred proton is bonded to nitrogen; one (3, -1) critical point (CP) being located between the two nuclei in iF and wF is observed. The  $\rho_{(3,-1)}$  (N-H) electron density decreases and drops down dramatically before entering the TS region (weakening bond).

Meanwhile,  $\rho_{(3,-1)}$  (O-H) CP is created between the hydrogen atom and the oxygen (strengthening bond) in wF, but in iF before TS region, the  $\rho_{(3,-1)}$  (N-H) disappears. The electron density at this second CP rapidly increases until the system gets out of the transition state region, the N-H (3, -1) CP being annihilated in iF. Thus, inside the TS region, both (N-H) and (H-O) CPs coexist. Then, as the consequence of the Poincaré–Hopf relationship, one (3, +1) RCP is equally present. The corresponding density at this (3, +1) CP begins to increase until reaching the TS where it takes its maximal value; then, it disappears at the frontier of the TS region in iF. Similar trends are observed for wF in which more bonds get involved, thus producing a ring critical point in all reaction regions, as observed in Fig. 6.

Figure 7 show the evolution of the Laplacian of electron density at the mentioned CPs, which serves as a way of

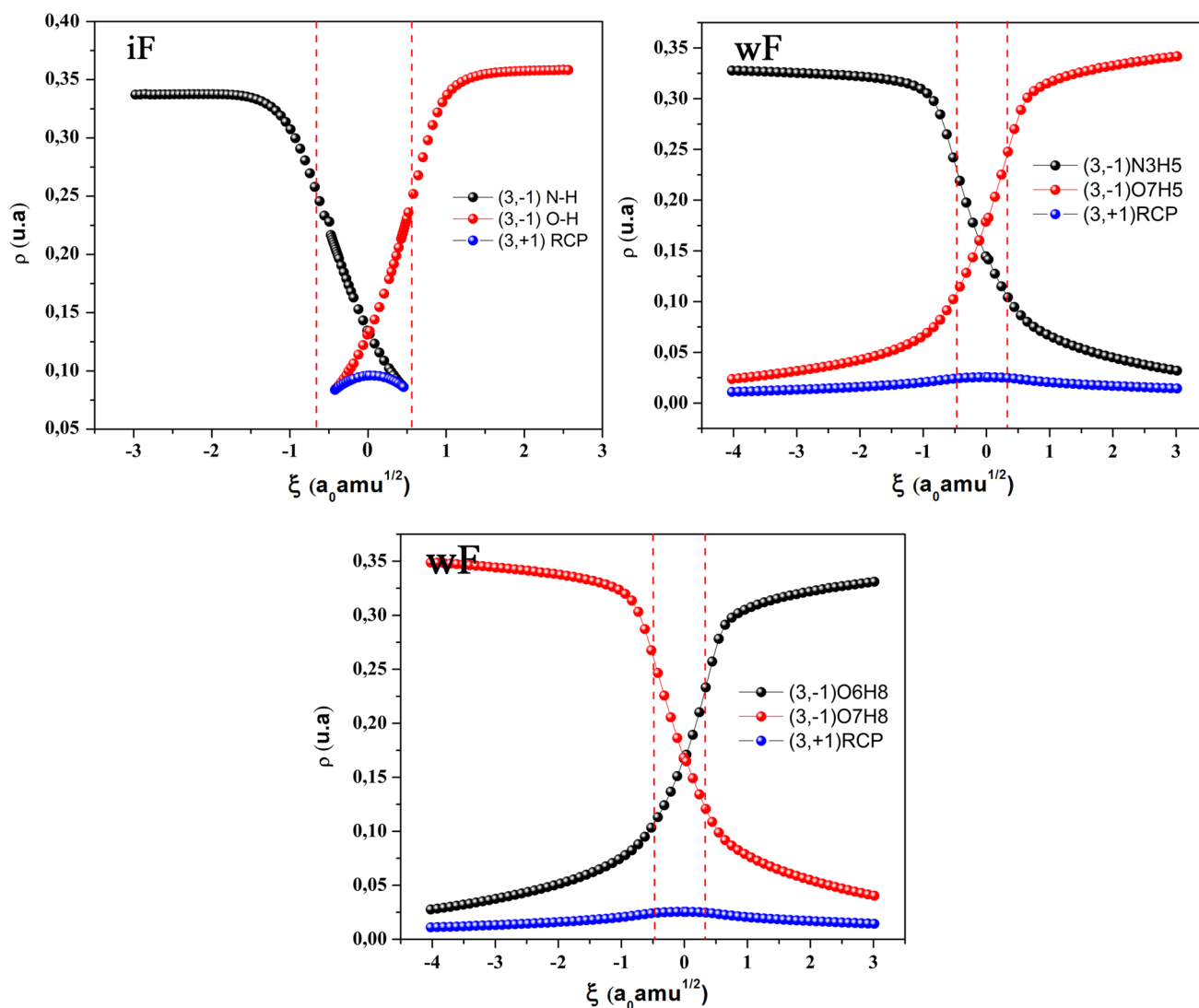


**Fig. 6** Electron density profiles at the selected  $(3, -1)$  and  $(3, +1)$  critical points with respect to the reaction coordinate describing proton transfer in iF and wF

characterizing the nature of the formed bonds. Both, intramolecular proton transfer reactions and water-mediated processes show that  $\nabla^2\rho_{(3,-1)}(\text{N-H})$  is negative; in some cases, it becomes positive within the TS region, in agreement with the covalent nature of the N-H interaction. It is important to stress that at the TS,  $\nabla^2\rho_{(3,-1)}(\text{N-H})$  becomes positive, which means that the nature of the N-H interaction has changed becoming more electrostatic. As intuitively expected, the exact opposite behavior is observed for  $\nabla^2\rho_{(3,-1)}(\text{H-O})$ , and as already observed for  $\nabla^2\rho_{(3,+1)}$ , it is maximal at the transition state; these results are in agreement with previous studies [44]. In water-mediated processes,  $\nabla^2\rho_{(3,+1)}$  shows a more peculiar behavior; it shows up in all reaction regions, indicating that the water molecule acts as a linker between the donor and acceptor atoms in the PT processes. In summary, the analysis of the

electron density (Fig. 6) provides a detailed characterization of the bond-breaking/bond-forming processes delimited by the emergence and annihilation of  $(3, -1)$  CPs. The Laplacian of electron density (Fig. 7) serves as a way of characterizing the nature of the bond; in all reactions, we have found that the nature of the interactions involved in the proton transfers changes from covalent bonds to electrostatic interaction and vice versa.

## 5 Conclusion

In this work, we have analyzed and characterized the mechanism of the intramolecular proton transfer reactions in formamide and thioformamide and the role of the water molecule in the chemical process at the DFT/B3LYP 6-311G\*\*



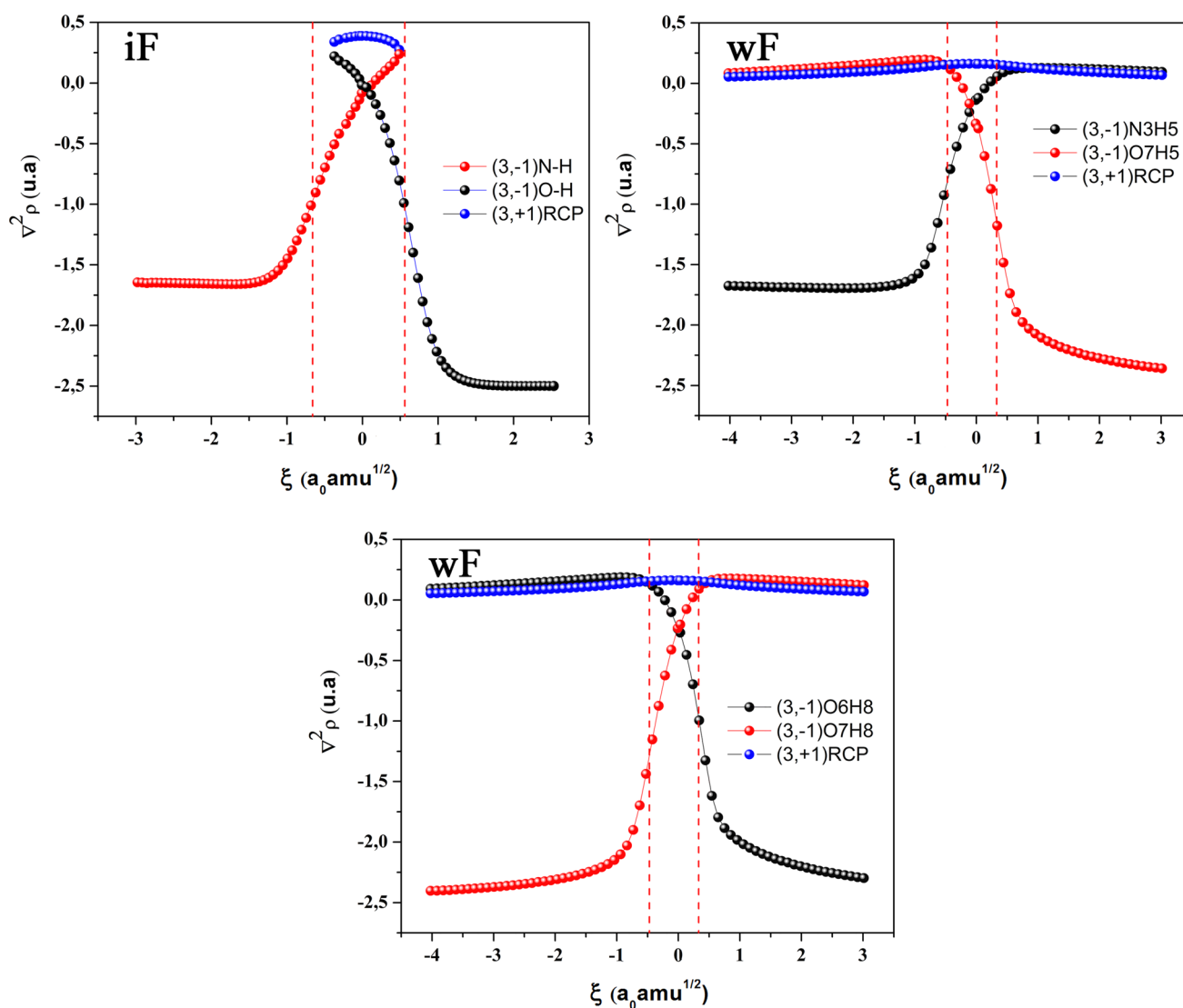


**Fig. 7** Laplacian of electron density profiles at the selected (3, -1) and (3, +1) critical points with respect to the reaction coordinate describing proton transfer in iF and wF

level of theory. We have completely characterized the systems through the analysis of energy, reaction force, reaction electronic flux, electronic population and Bader's quantum theory of atoms in molecules.

It was found that PT processes are thermodynamically unfavorable being in all cases the amino form more stable. The reaction force analysis helped quantify the electronic and structural contributions to the energy barriers; in all cases, the structural rearrangements were predominant. On the other hand, it has been shown that water molecule acts as a catalyst; energy barrier decreases by a factor of two in both reactions.

The use of the REF was useful to understand the nature of electronic activity and to identify when this

activity takes place along the reaction coordinate. In iPT, the strengthening and forming process are predominant. In wPT, the water molecule can modify the electronic activity; this change depends on the atomic substitution in the solute. The QTAIM topological analysis (BCPs and RCPs) allowed to characterize the electronic localization/delocalization processes during the proton transfer, elucidating the nature of the interactions involved that goes from covalent bonds to electrostatic interaction and vice versa.

**Acknowledgments** This work was supported by FONDECYT through project Nos. 1120093, 1100881 and 1130072. The authors acknowledge financial support from ICM through project No. 120082.

## References

- Bell RP (1980) *The tunnel effect in chemistry*. Chapman and Hall, New York
- Bender ML (1971) *Mechanisms of homogeneous catalysis from protons to proteins*. Wiley, New York
- Boutis T (1992) *Proton transfer in hydrogen bonded systems*. Plenum, New York
- Kim Y, Lim S, Kim HL, Kim Y (1999) *J Phys Chem A* 103:617
- Adamo C, Cossi M, Barone V (1997) *J Comput Chem* 18:1993
- Zielinski TJ, Poirier RA (1984) *J Comput Chem* 5:466
- Wang X-C, Nichols J, Feyereisen M, Gutowski M, Boatz J, Haymet ADJ, Simons J (1991) *J Phys Chem* 95:10419
- Duarte F, Toro-Labbé A (2010) *Mol Phys* 108:1375
- Hargis JC, Vöhringer-Martinez E, Lee Woodcock H, Toro-Labbé A, Schaefer HF III (2011) *J Phys Chem A* 115:2650
- Fu A, Li H, Du D, and Zhou Z (2003) *Chem Phys Lett* 382:332
- Markova N, Echev VJ (2004) *Mol. Struct. (Theochem)* 679:195
- Fujiwara S, Kambe N (2005) *Top Curr Chem* 251:87
- Vöhringer-Martinez E, Toro-Labbé A (2010) *J Comput Chem* 31:2642
- Bai LL, Yan SH, Ma HQ, Bi SW (2011) *Comput Theor Chem* 964:218
- Toro-Labbé A (1999) *J Phys Chem A* 103:4398
- Gutiérrez-Oliva S, Herrera B, Toro-Labbé A, Chermette H (2005) *J Phys Chem A* 109:1748
- Politzer P, Toro-Labbé A, Gutiérrez-Oliva S, Herrera B, Jaque P, Concha M, Murray J (2005) *J Chem Sci* 117:467
- Rincón E, Jaque P, Toro-Labbé A (2006) *J Phys Chem A* 110:9478
- Labet V, Morell C, Grand A, Toro-Labbé A (2008) *J Phys Chem A* 112:11487
- Herrera B, Toro-Labbé A (2007) *J Phys Chem A* 111:5921
- Echegaray E, Toro-Labbé A (2008) *J Phys Chem A* 112:11801
- Vogt-Geisse S, Toro-Labbé A (2009) *J Chem Phys* 130:244308
- Flores P, Gutiérrez-Oliva S, Silva E, Toro-Labbé A (2010) *THEOCHEM* 943:121
- Duarte F, Toro-Labbé AJ (2011) *Chem Phys A* 115:3050
- Inostroza-Rivera R, Herrera B, Toro-Labbé A (2014) *Phys Chem Chem Phys* 16:14489
- Bader RFW (1990) *Atoms in molecules: a quantum theory*. Oxford University Press, New York
- Popelier PLA (2000) *Atoms in molecules an introduction*. Prentice Hall, Upper Saddle River
- Brovarets' OO, Hovorun DM (2013) *J Comput Chem* 34:2577–2590
- Brovarets' OO, Zhurakivsky RO, Hovorun DM (2014) *J Comput Chem* 35:451–466
- Bonnet ML, Tognetti V (2011) *Chem Phys Lett* 511:427–433
- Parr RG, Yang W (1989) *Density functional theory of atoms and molecules*. Oxford University Press, New York
- Geerlings P, De Proft F, Langenaeker W (2003) *Chem Rev* 103:1793
- Morell C, Tognetti V, Bignon E, Dumont E, Hernandez-Haro N, Herrera B, Grand A, Gutiérrez-Oliva S, Joubert L, Toro-Labbé A (2015) *Theor Chem Acc* 134:133
- Becke A (1993) *J Chem Phys* 98:5648
- Lee C, Yang W, Parr R (1988) *Phys Rev B* 37:785
- Miehlich B, Savin A, Stoll H, Preuss H (1989) *Chem Phys Lett* 157:200
- Vosko S, Wilk L, Nusair M (1980) *Can J Phys* 58:1200
- Fukui K (1981) *Acc Chem Res* 14:363
- Schlegel GW, Scuseria HB, Robb GE, Cheeseman MA, Scalmani JR, Barone G, Mennucci V, Petersson B, Nakatsuji GA, Caricato H, Li M, Hratchian X, Izmaylov HP, Bloino AF, Zheng J, Sonnenberg G, Hada JL, Ehara M, Toyota M, Fukuda K, Hasegawa R, Ishida J, Nakajima M, Honda T, Kitao Y, Nakai O, Vreven H, Montgomery T, Peralta JA Jr, Ogliaro JE, Bearpark F, Heyd M, Brothers JJ, Kudin E, Staroverov KN, Kobayashi VN, Normand R, Raghavachari J, Rendell K, Burant A, Iyengar JC, Tomasi SS, Cossi J, Rega M, Millam N, Klene JM, Knox M, Cross JE, Bakken JB, Adamo V, Jaramillo C, Gomperts J, Stratmann R, Yazyev RE, Austin O, Cammi AJ, Pomelli R, Ochterski C, Martin JW, Morokuma RL, Zakrzewski K, Voth VG, Salvador GA, Dannenberg P, Dapprich JJ, Daniels S, Farkas AD, Foresman Ö, Ortiz JB, Cioslowski JV, Fox J, Frisch DJ, Trucks MJ (2009) *Gaussian 09 Revision A.1*. Gaussian Inc., Wallingford, CT
- Keith TA (2015) *Aimall* (version 15.05.18). TK Gristmill Software, Overland Park
- Giri S, Echegaray E, Ayers PW, Nunez AS, Lund F, Toro-Labbé A (2012) *J Phys Chem A* 116:10015
- Giri S, Inostroza-Rivera R, Herrera B, Nunez AS, Lund F, Toro-Labbé A (2014) *J Mol Model* 20(9):1–9
- Cerón M, Herrera B, Araya P, Gracia F, Toro-Labbé A (2011) *J Mol Model* 17:1625
- Inostroza-Rivera R, Yahia-Ouahmed M, Tognetti V, Joubert L, Herrera B, Toro-Labbé A (2015) *Phys Chem Chem Phys* 17:17797